PERGAMON

International Journal of Heat and Mass Transfer 45 (2002) 4899–4905

International Journal of HEAT and MASS TRANSFER

www.elsevier.com/locate/ijhmt

Technical Note

Measurements of turbulent mass transport of a circular wall jet

Herlina, Adrian Wing-Keung Law *

School of Civil and Environmental Engineering, Nanyang Technological University, Nanyang Avenue, Singapore 639798, Singapore

Received 18 April 2001; received in revised form 24 March 2002

Abstract

The results of a laboratory investigation on the turbulence characteristics of a circular three-dimensional turbulent wall jet are presented. Measurements were taken up to 50 nozzle diameters using combined particle image velocimetry and planar laser induced fluorescence. The results showed that the induced turbulence was still evolving in the present range and had not achieved similarity. While the turbulent intensity for both velocity and concentration increased downstream, the turbulent mass transport showed a decline over distance for both the streamwise and spanwise directions, implying weakening dispersion from the jet core.

Keywords: Wall jet; Particle image velocimetry; Planar laser induced fluorescence; Turbulence mixing

1. Introduction

The subject of three-dimensional turbulent wall jets has received a great deal of attention in the last few decades due to its importance as a fundamental phenomenon in wall-bounded shear flow, e.g. Sforza and Herbst [10]; [1,6–8]. It is now understood that the mean velocity distribution of the jet in a vertical cross-section consists of two distinct flow regions. The region between the wall and the point of maximum velocity is known as the boundary layer, while that above the maximum velocity point the free mixing region. Generally, the velocity scale of the streamwise and spanwise velocity profiles are represented by the maximum of their time average velocity, U_{mo} and U_m, respectively. The vertical length scale is taken as $z_{m/2}$ that is the z co-ordinate where the velocity has a value half of U_{mo} in the free mixing region. Similarly, the lateral length scale is represented by $y_{m/2}$ for a three-dimensional wall jet. A schematic sketch of the length scales is given in Fig. 1.

While previous investigations have elaborated on the mean velocity structure of the wall jet, studies on the related turbulent mixing properties are scarce. In this study, we employ a non-instrusive laser-imaging approach of combining particle image velocimetry (PIV) and planar laser induced fluorescence (PLIF) developed by Law and Wang [4], to capture the instantaneous velocity and concentration distribution inside the wall jet. Both the mean and turbulence properties of the flow are revealed and the turbulent mass transport, i.e. the cross-correlation between the turbulence velocity and concentration fluctuations, can also be determined since the measurements were synchronised. The distribution of the mean velocity and concentration had been presented in Law and Herlina [11]. In this note, we shall briefly summarise the turbulence properties. It will be shown that the turbulence characteristics were still evolving up to 50 diameter downstream. This is consistent with the observations by Padmanabham and Gowda [7] that similarity of the turbulence properties can only be achieved after $60d$. Thus, the present range does not extend to the fully developed region. The information should however be useful for future calibration of mathematical models towards evolving turbulent mass transfer in wall bounded shear flows.

* Corresponding author. Tel.: +65-6790-5296; fax: +65-6791-0676.

E-mail address: cwklaw@ntu.edu.sg (A.W.-K. Law).

0017-9310/02/$ - see front matter
PII: S0017-9310(02)00177-1

Nomenclature

c	instantaneous concentration
C	mean concentration
C_m	maximum concentration
C_{mo}	centreline maximum concentration
d	diameter of the nozzle
Re	discharge Reynolds number
u, v, w	instantaneous velocity in the x, y, z direction respectively
U, V, W	mean velocity in the x, y, z direction respectively
U_m	maximum velocity
U_{mo}	centreline maximum velocity
x, y, z	co-ordinates
$y_{cm/2}$	concentration-half-width
$y_{m/2}$	velocity-half-width
$z_{cm/2}$	concentration-half-height
$z_{m/2}$	velocity-half-height

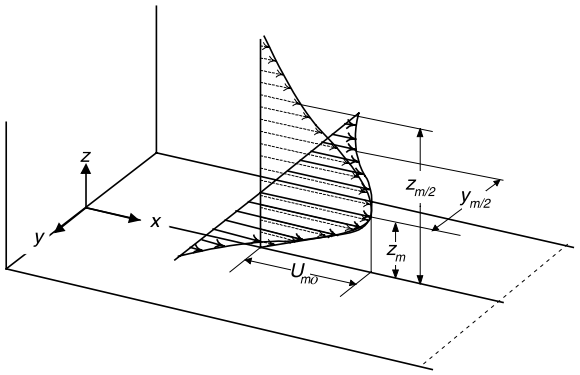

Fig. 1. Schematic diagram of the velocity structure of a three-dimensional wall jet.

2. Experiments

2.1. Experimental set-up

Experiments were performed in a glass tank with dimensions of 3 m length, 1 m width, and 1 m depth. A false sloping bottom made from perspex of 1.20 m length and 0.86 m width was submerged inside the tank and supported by a stainless steel framework. An aluminium nozzle with a diameter of 5.5 mm through which the discharge fluid entered the test tank was placed on top of the submerged floor. The nozzle had a wall thickness of 1 mm, hence the centre of the nozzle was situated at 3.75 mm above the bottom boundary. A separate mixing tank was used for the preparation and re-circulation of the discharges.

The detailed working for the combined PIV and PLIF had been given in [4] and is not repeated here. The arrangements of the equipment for the measurements in the streamwise and spanwise directions are illustrated in Fig. 2(a) and (b) respectively.

3. Streamwise turbulence characteristics

To detail the flow structure, velocity profiles along the centreline of the wall jet were captured up to $x/d = 50$ with three different discharge Reynolds numbers (Re) of 5500, 12,200, and 13,700 respectively. The Re should be large enough to yield a turbulent jet at the onset. Measurements were conducted at six imaging windows to cover this extensive range, with an overlap between two successive windows of about 10–20%. From each window, a total of 256 streamwise velocity profiles can be determined by collecting 300 instantaneous vector maps over a period of 1 min. They showed the typical mean flow structure of the wall jet with the two distinct flow regions. Note that the measurements did not extend to the wall surface because the accuracy of PIV deteriorated very close to the wall due to the reflection of laser light.

Fig. 3 shows the turbulence intensity distribution of the u-component at selected cross-sections with $Re = 12,200$. The turbulence intensity is computed as the standard deviation of the 300 instantaneous velocity vectors at a single location. The distribution profiles for other Re were similar and can be found in [3]. The data in Fig. 3 clearly show that the turbulence did not achieve similarity within the measurement range. Previous works by Newman et al. [5] (N72), Schwab [9] (S86), Fujisawa and Shirai [2] (FS89), Padmanabham and Gowda [7] (PG91), and Abrahamsson et al. [1] (AJL97) are included in the figure for comparison. The maximum turbulence intensity occurred at around $0.59z_{m/2}$ which is consistent with the other results. However, the magnitude of the maximum turbulence intensity differs among the different profiles. In particular, our measured peaks of the turbulence intensity were between 25% and 30% in good agreement with S86 and AJL97. On the other hand, PG91 and N72 showed considerably higher (35%) and lower (22%) value, respectively.

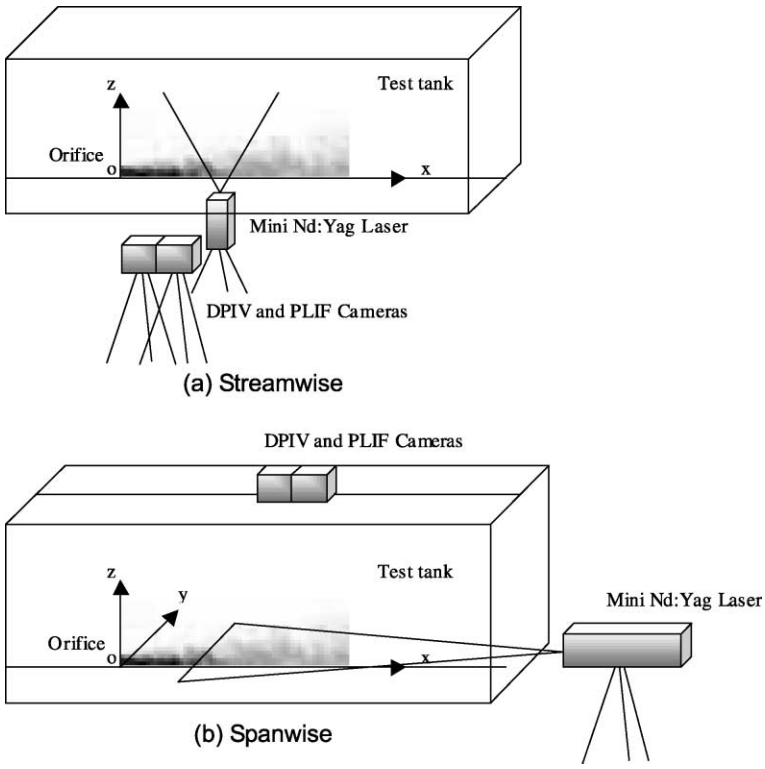

Fig. 2. Schematic illustration of the experimental set-up in (a) V-series and (b) H-series.

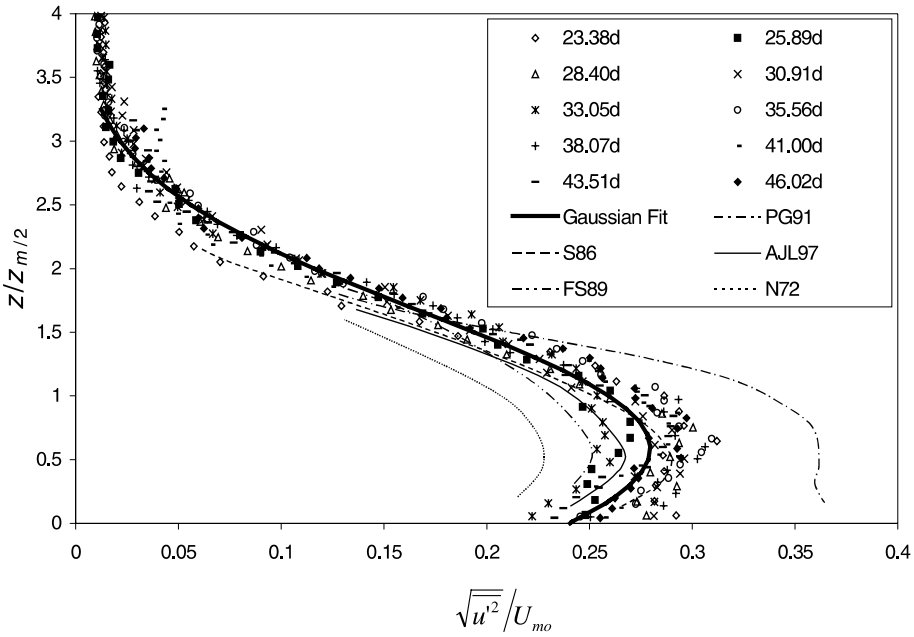

Fig. 3. Streamwise variation of u-component turbulence intensity (N72—[5], S86—[9], FS89—[2], PG91—[7], and AJL97—[1]).

The turbulence intensity of the w-component in Fig. 4 was found to be lower than the u-component. The peak was located around $0.8z_{m/2}$ with a maximum of approximately 18%. Comparison with previous results showed wider distribution with lower peak. It should however be noted that the accuracy of w-turbulence

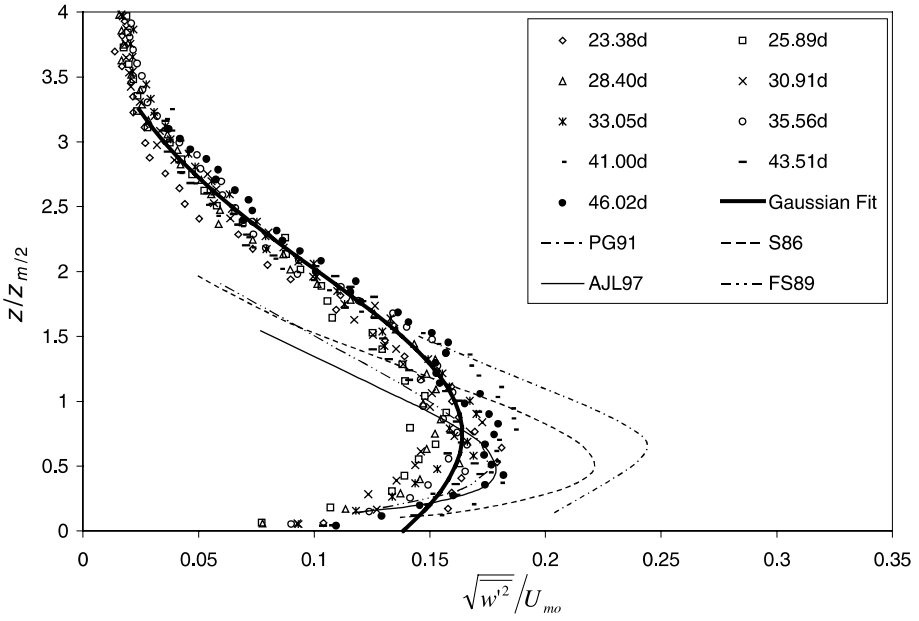

Fig. 4. Streamwise variation of w-component turbulence intensity.

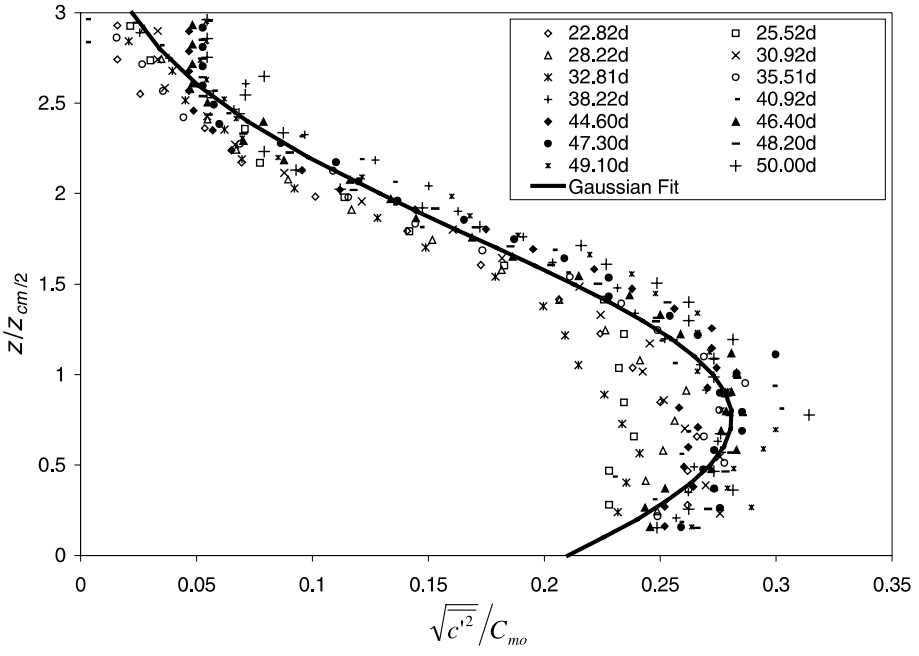

Fig. 5. Streamwise variation of concentration fluctuations.

intensity was poor due to the fact that the time interval between pulses for PIV was based on the axial u-component. This is a common problem for PIV in a flow with a predominant direction.

Fig. 5 shows the concentration turbulence intensity in the streamwise direction. In general, the intensity increased with the distance from the nozzle indicating again that the turbulence field was still evolving. At the farthest point measured ($x/d = 50$), the intensity increased from the wall up to a maximum of approximately 30% around $0.8z_{cm/2}$ and then decreased again.

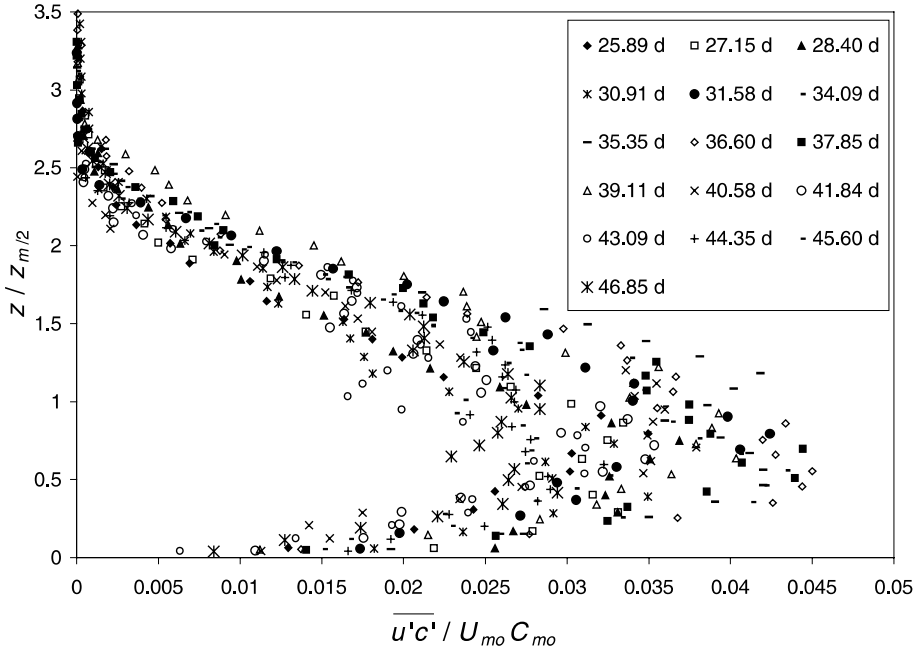

Fig. 6. Streamwise variation of turbulent mass transport.

The turbulent mass transport in the streamwise direction is shown in Fig. 6. It is interesting to point out that in general the turbulence intensities of both velocity and concentration increased with distance from the nozzle in the present range ($x/d = 20$–50) but their cross-correlation, the turbulent mass transport, decreased.

4. Spanwise turbulence characteristics

For spanwise experiments, the velocity measurements were taken at a height where the centre of the nozzle was located. It was anticipated that around that height the maximum velocities and concentrations would likely

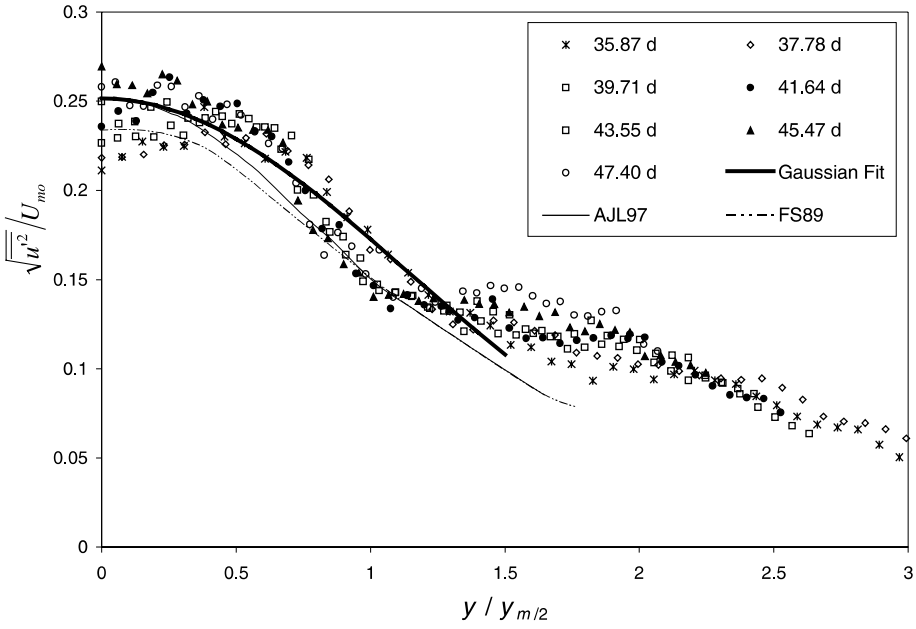

Fig. 7. Spanwise variation of u-component turbulence intensity.

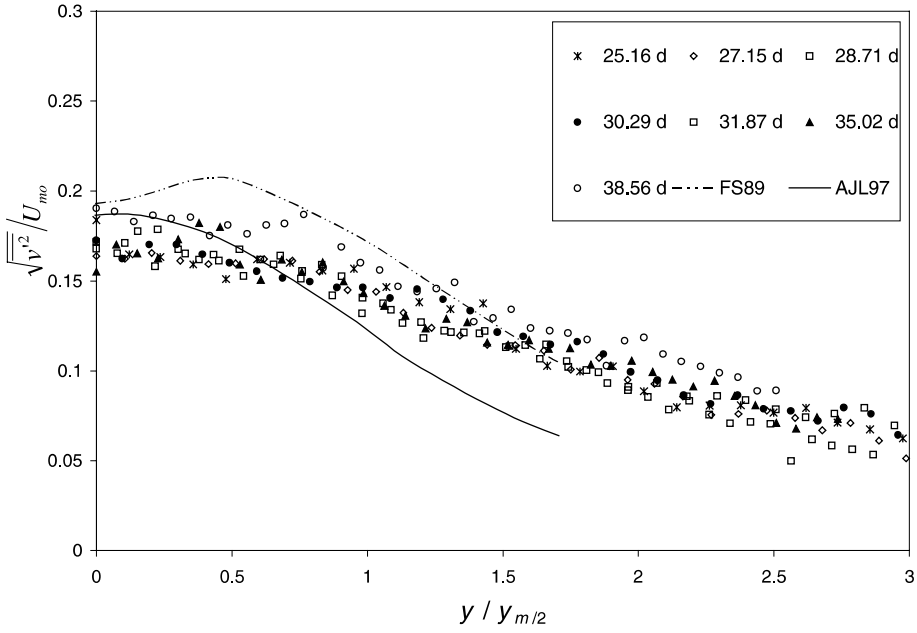

Fig. 8. Spanwise variation of v-component turbulence intensity at $z = z_m$.

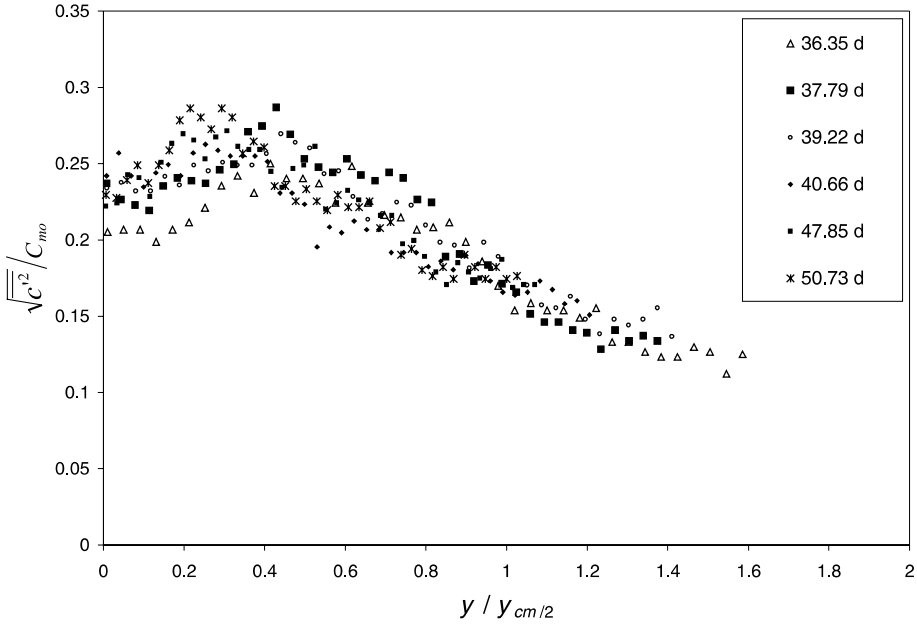

Fig. 9. Spanwise variation of concentration fluctuation at $z = z_m$.

occur. *Re* was the same as the streamwise experiments. DPIV were carried out at four imaging windows, with 10–20% overlap to cover a range up to $x/d = 50$. From each window, a total of 168 cross-sectional velocity profiles were obtained with 32×32 pixel interpolation.

The variation of u-turbulence intensity with $Re = 5500$ is shown in Fig. 7. Despite the fact that the turbulence field did not achieve similarity, the spanwise intensities were still in reasonable agreement with FS89 and AJL97. The maximum intensity was approximately

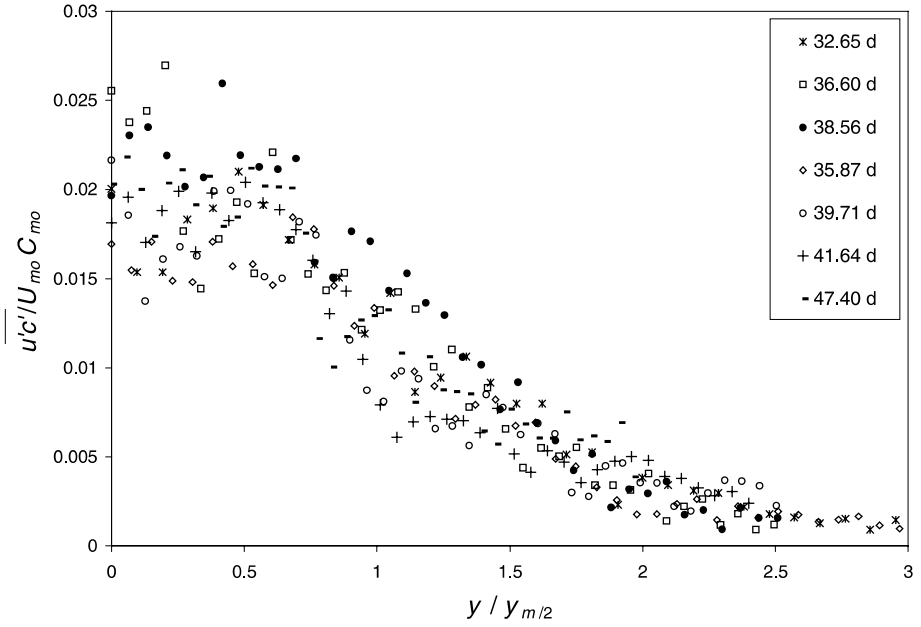

Fig. 10. Spanwise variation of turbulent mass transport at $z = z_m$.

26% occurring around the centre of the wall jet. On the other hand, the spanwise v-turbulence intensity (Fig. 8) showed a lower maximum of about 20% but at the same location. The data from 0 to $1.5y_{m/2}$ are in good agreement with FS89 and AJL97.

The concentration fluctuation intensity in the spanwise direction is shown in Fig. 9. It increased from the centreline of the jet up to approximately $0.3y_{cm/2}$ and then decreased again. The turbulence level near the centreline was about 24% and the maximum was around 28%.

Finally, the distribution of the turbulent mass transport in spanwise direction is shown in Fig. 10. The data were scattered but in general they showed the turbulent transport decreasing from the centreline.

5. Conclusion

A detailed experimental study was conducted to investigate the turbulence characteristics of a three-dimensional wall jet. The measurements showed that the induced turbulence was still evolving in the present range up to 50d downstream and did not achieve similarity. While the turbulence velocity and concentration intensity increased downstream, the turbulent mass transfer showed a decline over distance from the exit, implying weakening dispersion from the jet core.

References

[1] H. Abrahamsson, B. Johansson, L. Löfdahl, The turbulence field of a fully developed three-dimensional wall jet. Internal report 97/1, Department of Thermo and Fluid Dynamics, Chalmers University of Technology, Göteborg, Sweden, 1997.

[2] N. Fujisawa, H. Shirai, Mean flow and turbulence characteristics of three-dimensional wall jet along plane surface, Trans. Japan Soc. Aero. Space Sci. 32 (95) (1989) 35–46.

[3] Herlina, Mixing of Wall Jets and Gravity Plumes. MEng thesis, Nanyang Technological University, Singapore, 2000.

[4] A.W.K. Law, H.W. Wang, Measurements of Mixing Processes using Combined DPIV and PLIF, J. Expt. Thermal Fluid Sci. 22 (3–4) (2000) 213–229.

[5] B.G. Newman, R.P. Patel, S.B. Savage, H.K. Tjio, Three-dimensional wall jet originating from a circular orifice, Aeronaut. Quart. 23 (1972) 188–200.

[6] G. Padmanabham, B.H.L. Gowda, Mean and turbulence characteristics of a class of three-dimensional wall jets. Part 1. Mean flow characteristics, J. Fluids Eng. Trans. ASME 113 (1991a) 620–628.

[7] G. Padmanabham, B.H.L. Gowda, Mean and turbulence characteristics of a class of three-dimensional wall jets. Part 2. Turbulence characteristics, J. Fluids Eng. Trans. ASME 113 (4) (1991b) 629–634.

[8] N. Rajaratnam, B.S. Pani, Three-dimensional turbulent wall jets, J. Hydr. Div. ASCE 100 (1) (1974) 69–83.

[9] R.R. Schwab, A three-dimensional wall jet: Turbulence quantities. TFG/86/3, Department of Mechanical Engineering, Queen's University, Kingston, Ontario, Canada, 1986.

[10] P.M. Sforza, G. Herbst, A study of three-dimensional incompressible, turbulent wall jets, AIAA Journal 8 (2) (1970) 276–283.

[11] A.W.-K. Law, Herlina, An experimental study on turbulent circular wall jets, J. Hgd. Eng. 128 (2) (2002) 161–174.